H_∞ Bipartite Synchronization Composite Antidisturbance Control of Hidden Markov Jump Reaction–Diffusion Neural Networks

Xuelian Wang, Lin Sun, Yu-Long Wang, *Senior Member, IEEE*, and Tek Tjing Lie, *Life Senior Member, IEEE*

***Abstract*—This article investigates the problem of composite H_∞ control for cooperation–competition networks with hidden Markov jump parameters reaction–diffusions dynamics. Considering the difficulty of directly obtaining the mode information of systems, a continuous-time hidden Markov jump model is employed to represent the joint jump process. Specifically, the hidden process stands for the dynamics of real systems, which cannot be precisely known but can be observed through a detector. Due to the existence of multiple disturbances, the performance of the aforementioned systems can be deteriorated. To reduce the influence of these disturbances, a composite disturbance observer-based controller is constructed, which combines a disturbance observer with a feedback control mechanism. This design significantly improves the robustness and antidisturbance capability of systems. Then, sufficient criteria are derived to guarantee that the bipartite synchronization error system (BSES) is stochastically stable and meets a desired performance index. Finally, the effectiveness of the proposed control method is verified through the performance analysis.**

***Index Terms*—Bipartite synchronization, composite disturbance rejection control (CDRC), cooperation–competition networks, hidden Markov jump model, reaction–diffusion.**

NOMENCLATURE

Abbreviation	**Expansion**
$\mathbb{R}^n$	n-dimensional real vectors.
$\mathbb{R}^{m\times n}$	Set of $m \times n$ real matrices.
$\|\cdot\|$	Two-norm.
$\mathbb{R}^+$	Positive integers.
sgn$(\cdot)$	Sign function.
B^T	Transpose of matrix B.
$\otimes$	Kronecker product.
$\mathcal{E}\{\cdot\}$	Expectation operator.
$\hat{\lambda}_{\min}(\cdot)$	Minimum eigenvalue.
diag$\{\cdots\}$	Block diagonal matrix.
$*$	Symmetry of matrix blocks.
I_n	Identity matrix.
$\mathbf{1}_N$	Column vector with all entries being 1.
$B > 0(\geq 0)$	Positive (semipositive) definite and symmetric matrix.
$\Delta \triangleq \sum_{k=1}^{\varkappa}(\partial^2/\partial x_k^2)$	Laplace diffusion operator on Ω.

Received 30 September 2025; revised 29 November 2025; accepted 18 December 2025. This work was supported in part by the National Key Research and Development Program of China under Grant 2024YFB4707400; in part by the National Natural Science Foundation of China under Grant 52371372; and in part by the 111 Project, China under Grant D18003. This article was recommended by Associate Editor D. Diallo. *(Corresponding author: Yu-Long Wang.)*

Xuelian Wang and Yu-Long Wang are with the Shanghai Key Laboratory of Power Station Automation Technology and the School of Mechatronic Engineering and Automation, Shanghai University, Shanghai 200444, China (e-mail: xuelianwang@shu.edu.cn; yulongwang@shu.edu.cn).

Lin Sun is with Tianjin Key Laboratory of Intelligent Unmanned Swarm Technology and System, School of Electrical and Information Engineering, Tianjin University, Tianjin 300072, China (e-mail: sunlin1011_68@163.com).

Tek Tjing Lie is with the School of Engineering, Computer and Mathematical Sciences, Auckland University of Technology, Auckland 1010, New Zealand (e-mail: tek.lie@aut.ac.nz).

Color versions of one or more figures in this article are available at https://doi.org/10.1109/TCYB.2025.3647665.

Digital Object Identifier 10.1109/TCYB.2025.3647665

I. INTRODUCTION

IN THE last decade, synchronized control of coupled neural networks (CNNs) has received considerable attention, owing to its broad applicability in intelligent transportation, multiagent systems, secure communications, and more [1], [2], [3]. Typically, the interconnection among dynamic nodes in CNNs follows a specific topology, reflecting the information interaction among individual neurons. Note that prior research primarily concentrates on cooperative interactions among network nodes. However, the diversity of practical cases demands that competitive interactions should also be taken into account. Consequently, cooperative–competitive neural networks (CCNNs) have been increasingly investigated in recent years, see [4], [5], [6] and the references therein. In practice, sudden changes, for example, sensors with malfunctions, blocked actuators, variations in solar radiation, in the dynamic behavior of systems are inevitable [7], [8], [9]. These changes exhibit the Markov property to a certain extent, hence, allowing the system dynamics to be effectively modeled using a Markov chain [10]. In most existing results, the controller or filter is typically assumed to be fully accessible and synchronized with the system mode. For instance, the H_∞ bipartite synchronization control problem for a class of CCNNs with the Markov-switched topology is investigated in [11]. However, in dynamic networks, communication delays and asynchronous information sampling are often encountered, *making it difficult to ensure mode consistency between the system and the controller or filter*.

To address this issue, the hidden Markov model (HMM) has been presented as an efficient solution tool [12], [13], [14]. This model accounts for the case where real system dynamics, i.e., the Markov state, can not be directly observed. Consequently, the controller or filter is modeled based on an observed probability matrix obtained by an auxiliary detector. For example, the H_∞ control of continuous-time nonlinear hidden Markov jump systems subject to an interval type-2 fuzzy model is investigated in [15]. However, these studies commonly assume that network system modes are governed by ordinary differential equations (ODEs), which may not always be sufficient for capturing complex physical phenomena. In practical scenarios, the movement of electrons within an asymmetric electromagnetic field may introduce diffusion effects, which cannot be accurately described by ODEs. Consequently, it is more appropriate to model such systems using partial differential equations (PDEs). Considering this case, CCNNs with reaction–diffusion terms (RDTs) have recently gained increasing research attention [16], [17]. For instance, the study in [18] explores robust exponential stabilization for uncertain delay reaction–diffusion systems using sliding mode boundary control. Notably, some existing works still do not fully account for the effects of multidisturbance phenomena.

In reality, external disturbances are inevitable and can significantly degrade system performance, even leading to instability. To mitigate such effects, many control approaches have been proposed, such as H_∞ control theory [19], the event-triggered control method [20], and the disturbance observer-based control (DOBC) scheme [21]. Among these, the DOBC scheme has received extensive attention because of its practicality, high efficiency, and strong robustness, see [22], [23], [24]. This approach employs an observer to estimate the unknown disturbances. Based on the observer output, a feedforward compensator is integrated with traditional control strategies, resulting in a composite disturbance rejection control (CDRC) scheme that suppresses multiple types of disturbances and achieves the desired performance. For general classes of networks subject to those multiple disturbances, the CDRC strategy has proven to be effective in various applications [25], [26], [27], [28]. However, *the disturbance rejection problem becomes more complex in CCNNs, where consensus and synchronization under such environments are of paramount importance*.

In the aforementioned networks, the interactions among nodes can be described using a Laplacian matrix, which forms the foundation for analyzing consensus and synchronization behaviors. Note that bipartite consensus problems in multiagent systems with directed graph topologies are explored in [29]. For networks with structurally balanced cooperation–competition interactions, the nodes are typically divided into two mutually antagonistic subgroups. Among nodes in each subgroup, cooperative interactions prevail, while antagonistic relationships are established between different subgroups. The nodes within each subgroup asymptotically converge to a reference state with the same magnitude but opposite sign. This phenomenon, referred to as bipartite synchronization in CCNNs, has attracted considerable attention from researchers recently [30], [31], [32]. Although the CDRC strategy has demonstrated significant advantages in mitigating multiple disturbances, its application to CCNNs subject to both RDTs and multiple disturbances remains unexplored. *This highlights the urgent need for further investigation on the CDRC framework designed for improving dynamic behaviors of CCNNs.*

Motivated by the above discussion, this article studies the problem of bipartite synchronization for hidden Markov jump CCNNs with RDTs, under the CDRC framework. The main contributions of this article are summarized as follows.

1) The bipartite synchronization problem is investigated for hidden Markov jump reaction–diffusion networks that exhibit both cooperative and antagonistic interactions. Unlike traditional Markov jump models, the hidden Markov process is adopted to more accurately capture the unobservable mode transitions of real systems, thereby enhancing the practical applicability of the model.
2) To effectively address the effects of multiple disturbances, the CDRC strategy integrating a state-feedback control scheme with a disturbance observer is developed. The designed controller ensures the stochastic stability of synchronization error systems in the bipartite framework. In contrast to existing results [33], which focus solely on static output-feedback control, the proposed approach provides a more general and robust framework.
3) The proposed CDRC method can achieve improved disturbance attenuation and system performance in CCNNs compared with the traditional H_∞ control approach, as demonstrated in Section IV.

The remainder of this article is organized as follows. The problem formulation is presented in Section II. Section III provides the derivation of the designed composite controller for a bipartite synchronization error system (BSES). Section IV verifies the effectiveness of our developed method by the performance analysis. In the last, the conclusion is drawn in Section V.

Notations used in this article are listed in the nomenclature. For convenience, define $\vartheta_{t,x} \triangleq \vartheta(t,x)$.

II. Problem Formulation and Preliminaries

A. Graph Theory

Consider a signed directed graph describing the interaction topology of N mutually coupled nodes in the CNN with RDTs. The graph $\mathfrak{R}_{\wp_t} \triangleq (\mathfrak{I}, \aleph, \mathcal{H}_{\wp_t})$ with the switching topology includes three parts: a node set $\mathfrak{I} \triangleq \{1, 2, \ldots, N\}$, an edge set $\aleph \subseteq \mathfrak{I} \times \mathfrak{I}$, and a weighted adjacency matrix $\mathcal{H}_{\wp_t} \triangleq [h_{ij\wp_t}] \in \mathbb{R}^{N\times N}$, where $\wp_t \in \mathcal{M} \triangleq \{1, 2, \ldots, M\}$ is the switching signal. If $(j, i) \in \aleph$ is satisfied for node i and node j, it means $h_{ij\wp_t} \neq 0$, otherwise $h_{ij\wp_t} = 0$. Assume that there is no self-edge, i.e., $h_{ii\wp_t} = 0$. Here, the value of $h_{ij\wp_t}$ can be negative or positive. When $h_{ij\wp_t} < 0$, it means the competition, otherwise it stands for the cooperation. The graph $\mathfrak{R}_{\wp_t}$ consists of two subnetworks: the competition subnetwork $\mathfrak{R}^-_{\wp_t} \triangleq (\mathfrak{I}, \aleph^-, \mathcal{H}^-_{\wp_t})$ and the cooperation subnetwork $\mathfrak{R}^+_{\wp_t} \triangleq (\mathfrak{I}, \aleph^+, \mathcal{H}^+_{\wp_t})$.

A degree matrix is defined as $\mathcal{D}_{\wp_t} \triangleq \text{diag}\{\check{d}_{1\wp_t}, \ldots, \check{d}_{N\wp_t}\}$ with $\check{d}_{i\wp_t} \triangleq \sum_{j=1}^{N} |h_{ij\wp_t}|$ for $i \in \mathfrak{I}$. The Laplacian matrix $\mathcal{V}_{\wp_t} \triangleq [v_{ij\wp_t}]_{N\times N}$ of graph $\mathfrak{R}_{\wp_t}$ is defined as follows:

$$\mathcal{V}_{\wp_t} = \mathcal{D}_{\wp_t} - \mathcal{H}_{\wp_t}. \tag{1}$$

The following definition introduces an important concept in CCNNs: structural balance, which allows the node set $\mathfrak{I}$ to be decomposed into two subgroups.

Definition 1 [29]: The signed graph $\mathfrak{R}_{\wp_t}(\wp_t \in \mathcal{M})$ is structurally balanced subject to $\mathcal{H}_{\wp_t}$ if it has two disjoint node sets $\{\mathfrak{I}_1, \mathfrak{I}_2\}$, satisfying $\mathfrak{I}_1 \cup \mathfrak{I}_2 = \mathfrak{I}$ and $\mathfrak{I}_1 \cap \mathfrak{I}_2 = \varnothing$, such that $h_{ij\wp_t} \geq 0,\ \forall i, j \in \mathfrak{I}_\jmath (\jmath \in \{1,2\})$ for each $\wp_t \in \mathcal{M}$; otherwise, all $h_{ij\wp_t} \leq 0, \forall i \in \mathfrak{I}_\jmath, j \in \mathfrak{I}_{\bar{\jmath}} (\jmath, \bar{\jmath} \in \{1,2\})$ for each $\wp_t \in \mathcal{M}$. It is called structurally unbalanced, instead.

Lemma 1 [11]: Given that a signed graph $\mathfrak{R}_{\wp_t}$ is structurally balanced, as defined in Definition 1, a diagonal matrix $\bar{\mu} \triangleq \operatorname{diag}\{\mu_1, \mu_2, \ldots, \mu_N\}$ with $\mu_i \in \{1, -1\}$ for all $i \in \mathfrak{I}$ is introduced. Let $\breve{\mathcal{H}}_{\wp_t} \triangleq \bar{\mu}\mathcal{H}_{\wp_t}\bar{\mu}$, where $\breve{\mathcal{H}}_{\wp_t} \triangleq [|h_{ij\wp_t}|] \in \mathbb{R}^{N\times N}$. It follows that all entries of $\breve{\mathcal{H}}_{\wp_t}$ are nonnegative.

Remark 1: Note that the signed graph $\mathfrak{R}_{\wp_t}$ considered in this article is more general than traditional unsigned graphs. In such signed graphs, the corresponding Laplacian matrix generally does not possess the zero-row-sum property. To facilitate the analysis, a transformation matrix $\bar{\mu}$ is introduced (see Lemma 1), which allows for the construction of a modified Laplacian matrix $\breve{\mathcal{V}}_{\wp_t} \triangleq \bar{\mu}\mathcal{V}_{\wp_t}\bar{\mu} \triangleq [\breve{v}_{ij\wp_t}]_{N\times N}$ that satisfies the zero-row-sum property.

B. Node Dynamics Subject to the Switching Topology

Consider the CNN corresponding to hidden Markov jump parameters, RDTs, and antagonistic interactions. The dynamics of node i in this network are described by

$$\begin{aligned}\frac{\partial \vartheta_{i,t,x}}{\partial t} &= D_k \Delta \vartheta_{i,t,x} - A_{\wp_t}\vartheta_{i,t,x} + B_{\wp_t} f(\vartheta_{i,t,x}) \\ &\quad + C_{\wp_t}(u_{i,t,x} + d_{i,t,x}) + E_{i\wp_t} w_{t,x} \\ &\quad + c\sum_{j=1}^{N} |h_{ij\wp_t}|(\operatorname{sgn}(h_{ij\wp_t})\vartheta_{j,t,x} - \vartheta_{i,t,x}) \\ \bar{y}_{i,t,x} &= F_{\wp_t}\mu_i\vartheta_{i,t,x}, i = 1, 2, \ldots, N \end{aligned} \tag{2}$$

where $\vartheta_{i,t,x} \triangleq [\vartheta_{i1,t,x}, \ldots, \vartheta_{in,t,x}]^T \in \mathbb{R}^n$ denotes the state vector of node i at time t, and in space $x \in \Omega \subset \mathbb{R}^{\varkappa}$. For each node i, $u_{i,t,x} \in \mathbb{R}^{n_u}$ and $y_{i,t,x} \in \mathbb{R}^{n_y}$ represent the control input and the corresponding output signal, respectively; $f(\vartheta_{i,t,x}) \triangleq [f_1(\vartheta_{i1,t,x}), \ldots, f_n(\vartheta_{in,t,x})]^T \in \mathbb{R}^n$ is the activation function; $d_{i,t,x} \in \mathbb{R}^{n_u}$ represents the external disturbance modeled by an exogenous system; $w_{t,x} \in \mathcal{L}_2([0,\infty), \mathbb{R}^{n_w})$ denotes the disturbance; $D_k \triangleq \operatorname{diag}\{\hat{d}_{1k}, \ldots, \hat{d}_{nk}\} \in \mathbb{R}^{n\times n}$ is a positive transmission diffusion parameter; $A_{\wp_t} \triangleq \operatorname{diag}\{a_{1\wp_t}, \ldots, a_{n\wp_t}\} \in \mathbb{R}^{n\times n}$ with $a_{\iota\wp_t} > 0 (\iota = 1, 2, \ldots, n)$; $B_{\wp_t} \in \mathbb{R}^{n\times n}$, $C_{\wp_t} \in \mathbb{R}^{n\times n_u}$, $E_{i\wp_t} \in \mathbb{R}^{n\times n_w}$ and $F_{\wp_t} \in \mathbb{R}^{n_y\times n}$ are known constant matrices with appropriate sizes; $c \in (0, \infty)$ stands for the coupling strength.

Consider $\wp_t$ $(t \in \mathbb{R}^+)$, a Markov process that takes value in the set $\mathcal{M} \triangleq \{1, 2, \ldots, M\}$. The mode transition probabilities satisfy

$$\Pr(\wp_{t+\nabla} = q | \wp_t = \epsilon) = \begin{cases} \pi_{\epsilon q}\nabla + o(\nabla) q \neq \epsilon \\ 1 + \pi_{\epsilon\epsilon}\nabla + o(\nabla) q = \epsilon \end{cases} \tag{3}$$

where $\nabla > 0$ and $\lim_{\nabla\to 0}[o(\nabla)/\nabla] = 0$. $\pi_{\epsilon q} \geq 0$ denotes the transition rate (TR) and $\pi_{\epsilon\epsilon} = -\sum_{q\neq\epsilon}\pi_{\epsilon q}$, where $\forall \epsilon, q \in \mathcal{M}$. Besides, $\Pi = [\pi_{\epsilon q}]$ is the TR matrix. For simplicity, define $\wp_t = \epsilon$.

The initial condition and the Dirichlet boundary condition for network dynamics in (2) are specified as

$$\begin{aligned} \vartheta_{i,0,x} &= \phi_{i,x}, \quad x \in \Omega \\ \vartheta_{i,t,x} &= 0, \quad (t, x) \in [0, +\infty) \times \partial\Omega \end{aligned} \tag{4}$$

in which $i \in \mathfrak{I}$ and $\phi_{i,x}$ is a continuous and bounded function.

In this article, the unknown external disturbance $d_{i,t,x}$ is modeled by the following exogenous system

$$\begin{aligned} \frac{\partial \eta_{i,t,x}}{\partial t} &= A_{d\epsilon}\eta_{i,t,x} + B_{di\epsilon}\omega_{t,x} \\ d_{i,t,x} &= C_{d\epsilon}\eta_{i,t,x} \end{aligned} \tag{5}$$

where $\eta_{i,t,x} \in \mathbb{R}^{n_\eta}$ denotes the state for $i \in \mathfrak{I}$; $\omega_{t,x} \in \mathcal{L}_2([0,\infty), \mathbb{R}^{n_\omega})$ is an additional disturbance caused by exogenous signals, which may lead to uncertainties and perturbations in the exogenous system; $A_{d\epsilon} \in \mathbb{R}^{n_\eta\times n_\eta}, B_{di\epsilon} \in \mathbb{R}^{n_\eta\times n_\omega}$, and $C_{d\epsilon} \in \mathbb{R}^{n_u\times n_\eta}$ are known matrices with matching dimensions.

Remark 2: It should be noted that multiple disturbances are considered in network dynamics (2), i.e., matched and mismatched disturbances. The matched disturbance $d_{i,t,x}$ can be generated by the exogenous system (5), which is assumed to be harmonic with a known frequency while its phase and magnitude remain unknown. Besides, to reflect the practical situation, an additional disturbance $\omega_{t,x}$ is also introduced into system (5). Therefore, multidisturbance phenomenon is addressed in this article.

Considering the unforced isolated node of network dynamics described in (2), the dynamic is given by

$$\begin{aligned} \frac{\partial \mathcal{T}_{t,x}}{\partial t} &= D_k\Delta\mathcal{T}_{t,x} - A_\epsilon\mathcal{T}_{t,x} + B_\epsilon f(\mathcal{T}_{t,x}) \\ \breve{y}_{t,x} &= F_\epsilon\mathcal{T}_{t,x} \end{aligned} \tag{6}$$

where $\mathcal{T}_{t,x} \in \mathbb{R}^n$ and $\breve{y}_{t,x} \in \mathbb{R}^{n_y}$ are the state vector and output vector of the isolated node, respectively.

The initial and the Dirichlet boundary conditions of the isolated node dynamic (6) are defined as

$$\begin{aligned} \mathcal{T}_{0,x} &= \breve{\phi}_x, \quad x \in \Omega \\ \mathcal{T}_{t,x} &= 0, \quad (t, x) \in [0, +\infty) \times \partial\Omega \end{aligned} \tag{7}$$

with $\breve{\phi}_x$ being continuous and bounded on Ω.

Define $\bar{\vartheta}_{i,t,x} \triangleq \mu_i\vartheta_{i,t,x}$ for $i \in \mathfrak{I}$. Using the property of the diagonal matrix $\bar{\mu}$, one has $\breve{\mathcal{V}}_\epsilon = \bar{\mu}\mathcal{V}_\epsilon\bar{\mu}$ for each $\epsilon \in \mathcal{M}$, where $\breve{\mathcal{V}}_\epsilon$ expresses the zero-row-sum matrix. Then, the CNN with switching topologies and RDTs can be reformulated as

$$\begin{aligned} \frac{\partial \bar{\vartheta}_{i,t,x}}{\partial t} &= D_k\Delta\bar{\vartheta}_{i,t,x} - A_\epsilon\bar{\vartheta}_{i,t,x} + B_\epsilon f(\bar{\vartheta}_{i,t,x}) + \mu_i E_{i\epsilon} w_{t,x} \\ &\quad + \mu_i C_\epsilon\left(u_{i,t,x} + d_{i,t,x}\right) - c\sum_{j=1}^{N}\breve{v}_{ij\epsilon}\bar{\vartheta}_{j,t,x} \\ \bar{y}_{i,t,x} &= F_\epsilon\bar{\vartheta}_{i,t,x}, i = 1, 2, \ldots, N. \end{aligned} \tag{8}$$

Define $e_{i,t,x} \triangleq \bar{\vartheta}_{i,t,x} - \mathcal{T}_{t,x}$, where $i \in \mathfrak{I}$. By synthesizing (6) and (8), the BSES is given by

$$\begin{aligned} \frac{\partial e_{i,t,x}}{\partial t} &= D_k\Delta e_{i,t,x} - A_\epsilon e_{i,t,x} + B_\epsilon f(e_{i,t,x}) + \mu_i E_{i\epsilon} w_{t,x} \\ &\quad + \mu_i C_\epsilon u_{i,t,x} + \mu_i C_\epsilon d_{i,t,x} - c\sum_{j=1}^{N}\breve{v}_{ij\epsilon} e_{j,t,x} \end{aligned}$$

$$y_{i,t,x} = F_\epsilon e_{i,t,x}, i = 1, 2, \ldots, N \tag{9}$$

where $f(e_{i,t,x}) \triangleq f(\bar{\vartheta}_{i,t,x}) - f(\mathcal{T}_{t,x})$.

C. Hidden Markov Jump Model

Consider a probability space $(\Omega, \mathcal{F}, \Pr)$. Let $\hbar_t = (\wp_t, \hat{\wp}_t)$ denotes the right continuous-time HMM, where $\wp_t$ represents the hidden state, $\hat{\wp}_t$ denotes the observation state taking values in the set $\mathcal{W} = \{1, 2, \ldots, W\}$, and $t \in \mathbb{R}^+$. Assume that $\hbar_t$ is a homogeneous Markov process taking values in the set $\mathcal{M} \times \mathcal{W}$. Then, one obtains that

$$\begin{aligned}&\Pr(\hbar_{t+\nabla} = (q, \delta) | \hbar_t = (\epsilon, \sigma)) \\ &\quad= \begin{cases} \rho_{(\epsilon,\sigma)(q,\delta)}\nabla + o(\nabla)(q, \delta) \neq (\epsilon, \sigma) \\ 1 + \rho_{(\epsilon,\sigma)(q,\delta)}\nabla + o(\nabla)(q, \delta) = (\epsilon, \sigma) \end{cases}\end{aligned} \tag{10}$$

where the TR $\rho_{(\epsilon,\sigma)(q,\delta)}$ satisfies

$$\rho_{(\epsilon,\sigma)(q,\delta)} = \begin{cases} \alpha^\sigma_{q\delta}\beta_{\epsilon q}, & q \neq \epsilon \\ \lambda^\epsilon_{\sigma\delta}, & q = \epsilon, \delta \neq \sigma \\ \beta_{\epsilon\epsilon} + \lambda^\epsilon_{\sigma\delta}, & q = \epsilon, \delta = \sigma \\ 0, & \text{otherwise} \end{cases} \tag{11}$$

while $\alpha^\sigma_{q\delta}$ represents the detection probability satisfying $\sum_{\delta=1}^{W} \alpha^\sigma_{q\delta} = 1; \beta_{\epsilon q} \geq 0$ stands for the TR for all $q \neq \epsilon$; $\lambda^\epsilon_{\sigma\delta} \geq 0$ represents the jumps of $\hat{\wp}_t$ when the mode of $\wp_t$ does not vary for all $\delta \neq \sigma$; and $\beta_{\epsilon\epsilon} = -\sum_{q\neq\epsilon}\beta_{\epsilon q}$, $\lambda^\epsilon_{\sigma\sigma} = -\sum^\epsilon_{\delta\neq\sigma}\lambda^\epsilon_{\sigma\delta}$. Assume that $\hat{\wp}_t$ is directly measured by a detector and regarded as the estimate of $\wp_t$. Define $\Pi^\sigma_\alpha, \Pi_\beta$, and Π^ϵ_λ as the detection probability matrix, the TR matrix of system, and the TR matrix of detector, respectively. For simplicity, let $\hat{\wp}_t \triangleq \sigma$.

Remark 3: In accordance with (11), the TR $\rho_{(\epsilon,\sigma)(q,\delta)}$ satisfies the following condition:

$$\begin{aligned} -\rho_{(\epsilon,\sigma)(q,\delta)} &= \sum_{q\neq\epsilon}\sum_{\delta=1}^{W}\rho_{(\epsilon,\sigma)(q,\delta)} + \sum_{\delta\neq\sigma}\rho_{(\epsilon,\sigma)(\epsilon,\delta)} \\ &= \sum_{q\neq\epsilon}\sum_{\delta=1}^{W}\alpha^\sigma_{q\delta}\beta_{\epsilon q} + \sum_{\delta\neq\sigma}\lambda^\epsilon_{\sigma\delta} \\ &= -\beta_{\epsilon\epsilon} - \lambda^\epsilon_{\sigma\delta}. \end{aligned}$$

Remark 4: Compared with the HMM-based framework adopted in [34], which enforces a strict correspondence between the controller and the system modes, the proposed approach allows for more flexible and adaptive control strategies. In practice, accurately obtaining the real-time mode of the original system is often challenging due to uncertainties or measurement limitations. To address this, instead of assuming full mode observability considered in [34], we employ a detector-based mechanism to estimate the mode transitions. This allows the controller mode to switch independently of the actual system mode, thereby enabling more practical and flexible controller design.

D. Disturbance Observer Construction

A disturbance observer is designed to estimate the unknown external disturbance $d_{i,t,x}$ described by (5). It is incorporated as a feedforward component in the composite controller to attenuate the effects of the external disturbance.

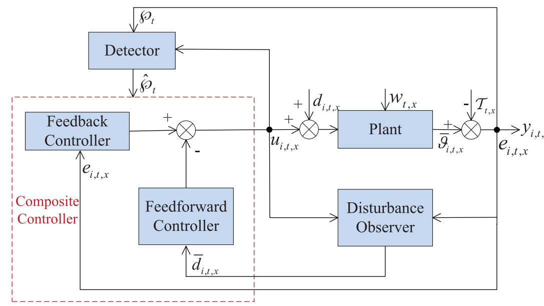

Fig. 1. Architecture of the detector-based CDRC mechanism.

The following disturbance observer is introduced to obtain the estimate of $d_{i,t,x}$ in the exogenous system (5):

$$\begin{aligned} \bar{d}_{i,t,x} &= C_{d\epsilon}\bar{\eta}_{i,t,x} \\ \bar{\eta}_{i,t,x} &= \check{\vartheta}_{i,t,x} - L_{i,\sigma}e_{i,t,x} \\ \frac{\partial\check{\vartheta}_{i,t,x}}{\partial t} &= (A_{d\epsilon} + \mu_i L_{i,\sigma}C_\epsilon C_{d\epsilon})(\check{\vartheta}_{i,t,x} - L_{i,\sigma}e_{i,t,x}) \\ &\quad + L_{i,\sigma}\big[D_k\Delta e_{i,t,x} - A_\epsilon e_{i,t,x} + B_\epsilon f(e_{i,t,x}) \\ &\quad - c\sum_{j=1}^{N}\check{v}_{ij\epsilon}e_{j,t,x} + \mu_i C_\epsilon u_{i,t,x}\big] \end{aligned} \tag{12}$$

where $\check{\vartheta}_{i,t,x} \in \mathbb{R}^{n_\eta}$ denotes an auxiliary vector variable with $i \in \mathfrak{I}$; $\bar{d}_{i,t,x} \in \mathbb{R}^{n_u}$ and $\bar{\eta}_{i,t,x} \in \mathbb{R}^{n_\eta}$ are disturbance estimates of $d_{i,t,x}$ and $\eta_{i,t,x}$, respectively; $L_{i,\sigma} \in \mathbb{R}^{n_\eta\times n}$ denotes the observer gain to be designed for $\sigma \in \mathcal{W}$.

E. Composite Controller Design

This article aims to propose a control scheme such that the external disturbance $d_{i,t,x}$ can be rejected and the composite system (16) is stochastically stable and satisfies the desired performance. A composite control scheme, integrating with the feedforward and feedback controllers, is introduced to attenuate different disturbances. The framework of the detector-based CDRC scheme is plotted in Fig. 1.

An appropriate composite control law for node i is designed as

$$u_{i,t,x} = K_{i,\sigma}e_{i,t,x} - \bar{d}_{i,t,x} \tag{13}$$

in which $K_{i,\sigma} \in \mathbb{R}^{n_u\times n}, i \in \mathfrak{I}, \sigma \in \mathcal{W}$, is the controller gain matrix to be determined later; $\bar{d}_{i,t,x}$ is applied to compensate the external disturbance of the ith node.

Remark 5: For the matched disturbance $d_{i,t,x}, i \in \mathfrak{I}$, in network dynamics (2), the DOBC method is established to actively reject the disturbance by incorporating the disturbance estimate $\bar{d}_{i,t,x}$ into the controller (13). In addition, the H_∞ control approach is employed to attenuate mismatched disturbance $w_{t,x}$. Thus, the proposed CDRC scheme is more adaptable and effective for network dynamics subject to multiple disturbances.

F. Composite System Modeling

Define $e_{\bar{\eta},i,t,x} \triangleq \eta_{i,t,x} - \bar{\eta}_{i,t,x}, i \in \mathfrak{I}$. By integrating (5) and (12), the BSES and estimation error system can be derived as follows:

$$\begin{aligned}\frac{\partial e_{t,x}}{\partial t} &= \hat{D}_k \Delta e_{t,,x} + \hat{A}_\epsilon e_{t,x} + \hat{B}_\epsilon f(e_{t,x}) \\ &\quad + \hat{C}_\epsilon e_{\bar{\eta},t,x} + \hat{E}_\epsilon w_{t,x} \qquad (14)\\ \frac{\partial e_{\bar{\eta},t,x}}{\partial t} &= (\hat{A}_{d\epsilon} + \hat{L}_\sigma \hat{C}_\epsilon) e_{\bar{\eta},t,x} + \hat{B}_{d\epsilon}\omega_{t,x} + \hat{L}_\sigma \hat{E}_\epsilon w_{t,x} \\ y_{t,x} &= \hat{F}_\epsilon e_{t,x} \qquad (15)\end{aligned}$$

with

$$\begin{aligned}\hat{B}_{d\epsilon} &\triangleq \left[\, B_{d1\epsilon}^T \; B_{d2\epsilon}^T \cdots B_{dN\epsilon}^T \,\right]^T \\ \bar{y}_{t,x} &\triangleq \left[\, \bar{y}_{1,t,x}^T \; \bar{y}_{2,t,x}^T \cdots \bar{y}_{N,t,x}^T \,\right]^T \\ \eta_{t,x} &\triangleq \left[\, \eta_{1,t,x}^T \; \eta_{2,t,x}^T \cdots \eta_{N,t,x}^T \,\right]^T \\ \bar{\eta}_{t,x} &\triangleq \left[\, \bar{\eta}_{1,t,x}^T \; \bar{\eta}_{2,t,x}^T \cdots \bar{\eta}_{N,t,x}^T \,\right]^T \\ \bar{\vartheta}_{t,x} &\triangleq \left[\, \bar{\vartheta}_{1,t,x}^T \; \bar{\vartheta}_{2,t,x}^T \cdots \bar{\vartheta}_{N,t,x}^T \,\right]^T \\ f\left(\bar{\vartheta}_{t,x}\right) &\triangleq \left[\, f^T\left(\bar{\vartheta}_{1,t,x}\right) \cdots f^T\left(\bar{\vartheta}_{N,t,x}\right) \right]^T \\ \hat{E}_\epsilon &\triangleq \check{\mu}\left[\, E_{1\epsilon}^T \; E_{2\epsilon}^T \cdots E_{N\epsilon}^T \,\right]^T, \quad \check{\mu} \triangleq \bar{\mu} \otimes I_n \\ f\left(e_{t,x}\right) &\triangleq f\left(\bar{\vartheta}_{t,x}\right) - \mathbf{1}_N \otimes f\left(\mathcal{T}_{t,x}\right), \quad e_{\bar{\eta},t,x} \triangleq \eta_{t,x} - \bar{\eta}_{t,x} \\ e_{t,x} &\triangleq \bar{\vartheta}_{t,x} - \mathbf{1}_N \otimes \mathcal{T}_{t,x}, \quad y_{t,x} \triangleq \bar{y}_{t,x} - \mathbf{1}_N \otimes \check{y}_{t,x} \\ \hat{A}_\epsilon &\triangleq I_N \otimes (-A_\epsilon) - c\left(\check{\mathcal{V}}_\epsilon \otimes I_n\right) + (I_N \otimes C_\epsilon)\check{\mu}\mathcal{K}_\sigma \\ \hat{D}_k &\triangleq I_N \otimes D_k, \quad \hat{C}_\epsilon \triangleq \bar{\mu} \otimes C_\epsilon C_{d\epsilon}, \quad \hat{B}_\epsilon \triangleq I_N \otimes B_\epsilon \\ \hat{F}_\epsilon &\triangleq I_N \otimes F_\epsilon, \quad \hat{A}_{d\epsilon} \triangleq I_N \otimes (A_{d\epsilon}), \quad \hat{B}_{d\epsilon} \triangleq I_N \otimes B_{d\epsilon} \\ \hat{L}_\sigma &\triangleq \mathrm{diag}\left\{L_{1,\sigma}, \ldots, L_{N,\sigma}\right\} \\ \mathcal{K}_\sigma &\triangleq \mathrm{diag}\left\{K_{1,\sigma}, \ldots, K_{N,\sigma}\right\}.\end{aligned}$$

Combining (14) with (15), the composite system can be formulated as follows:

$$\begin{aligned}\frac{\partial \zeta_{t,x}}{\partial t} &= \mathscr{D}_k \Delta \zeta_{t,x} + \mathscr{A}_\epsilon \zeta_{t,x} + \mathscr{B}_\epsilon f(e_{t,x}) + \mathscr{C}_\epsilon \Gamma_{t,x} \\ y_{t,x} &= \mathscr{F}_\epsilon \zeta_{t,x} \qquad (16)\end{aligned}$$

with

$$\begin{aligned}&\zeta_{t,x} \triangleq \left[\, e_{t,x}^T \quad e_{\bar{\eta},t,x}^T \,\right]^T, \Gamma_{t,x} \triangleq \left[\, w_{t,x}^T \quad \omega_{t,x}^T \,\right]^T \\ &\mathscr{D}_k \triangleq \begin{bmatrix} \hat{D}_k & 0 \\ 0 & 0 \end{bmatrix}, \mathscr{B}_\epsilon \triangleq \begin{bmatrix} \hat{B}_\epsilon \\ 0 \end{bmatrix}, \mathscr{F}_\epsilon \triangleq \left[\, \hat{F}_\epsilon \quad 0 \,\right] \\ &\mathscr{A}_\epsilon \triangleq \begin{bmatrix} \hat{A}_\epsilon & \hat{C}_\epsilon \\ 0 & (\hat{A}_{d\epsilon} + \hat{L}_\sigma \hat{C}_\epsilon) \end{bmatrix}, \mathscr{C}_\epsilon \triangleq \begin{bmatrix} \hat{E}_\epsilon & 0 \\ \hat{L}_\sigma \hat{E}_\epsilon & \hat{B}_{d\epsilon} \end{bmatrix}.\end{aligned}$$

Remark 6: Given that $w_{t,x} \in \mathcal{L}_2[0,\infty)$ and one can deduce that $\Gamma_{t,x} \in \mathcal{L}_2[0,\infty)$, which implies that disturbances are norm bounded.

Next, for the convenience of the analysis, we will introduce the following assumption and definitions.

Assumption 1: Suppose that the pairs (A_ϵ, C_ϵ) and $(A_{d\epsilon}, C_\epsilon C_{d\epsilon})$ are controllable and observable, respectively, where the matrix C_ϵ has the full column rank.

Definition 2: [16] For arbitrary initial conditions, the composite system (16), subject to Dirichlet boundary conditions, is stochastically stable with $\Gamma_{t,x} \equiv 0$, if the following condition is satisfied:

$$\lim_{t_f \to \infty} \mathcal{E}\left\{\int_0^{t_f} \|e_{t,x}\|^2 dt\right\} < \infty. \qquad (17)$$

Definition 3: [11] Given the gauge transformation matrix $\bar{\mu} \triangleq \mathrm{diag}\{\mu_1, \mu_2, \ldots, \mu_N\}$, where $\mu_i \in \{1, -1\}$ and $i \in \mathfrak{I}$, the bipartite synchronization is ensured for network dynamics (2) and (6), if the following condition is satisfied:

$$\lim_{t\to\infty} \mathcal{E}\left\{\|\mu_i \vartheta_{i,t,x} - \mathcal{T}_{t,x}\|\right\} = 0. \qquad (18)$$

III. Main Results

The bipartite synchronization control issue in view of the CDRC method is investigated. According to Theorem 1, some criteria describing the stability and H_∞ performance of the composite system (16) are obtained. Specific formulations of designed controller gains are presented in Theorem 2.

A. Stabilization and Performance Analysis

Theorem 1: If there exist positive definite diagonal matrices $P_{1\epsilon,\sigma} \in \mathbb{R}^{n\times n}$ and $P_{2\epsilon,\sigma} \in \mathbb{R}^{n_\eta \times n_\eta}$ such that the following conditions hold for all $\epsilon \in \mathcal{M}$ and $\sigma \in \mathcal{W}$

$$I_N \otimes (P_{1\epsilon,\sigma} D_k + D_k^T P_{1\epsilon,\sigma}) > 0 \qquad (19)$$

$$\bar{\Xi}_{\epsilon,\sigma} \triangleq \begin{bmatrix} \bar{\Xi}_{\epsilon,\sigma}^{1,1} & \bar{\Xi}_{\epsilon,\sigma}^{1,2} \\ * & \bar{\Xi}_{\epsilon,\sigma}^{2,2} \end{bmatrix} < 0 \qquad (20)$$

$$\Xi_{\epsilon,\sigma} \triangleq \begin{bmatrix} \Xi_{\epsilon,\sigma}^{1,1} & \bar{\Xi}_{\epsilon,\sigma}^{1,2} & \bar{\Xi}_{\epsilon,\sigma}^{1,3} & 0 \\ * & \bar{\Xi}_{\epsilon,\sigma}^{2,2} & \Xi_{\epsilon,\sigma}^{2,3} & \Xi_{\epsilon,\sigma}^{2,4} \\ * & * & -\gamma^2 I_{n_w} & 0 \\ * & * & * & -\gamma^2 I_{n_\omega} \end{bmatrix} < 0 \qquad (21)$$

with

$$\begin{aligned}\bar{\Xi}_{\epsilon,\sigma}^{1,1} &\triangleq I_N \otimes \left(\hat{\mathcal{D}}_{\epsilon,\sigma} + P_{1\epsilon,\sigma} B_\epsilon B_\epsilon^T P_{1\epsilon,\sigma} + \Phi + \bar{P}_{1q,\delta}\right) \\ &\quad - 2\left(I_N \otimes \left(P_{1\epsilon,\sigma} A_\epsilon\right) + c\left(\check{\mathcal{V}}_\epsilon \otimes P_{1\epsilon,\sigma}\right)\right. \\ &\quad \left. - \left(I_N \otimes P_{1\epsilon,\sigma} C_\epsilon\right)\check{\mu}\mathcal{K}_\sigma\right) \\ \Xi_{\epsilon,\sigma}^{1,1} &\triangleq \bar{\Xi}_{\epsilon,\sigma}^{1,1} + I_N \otimes F_\epsilon^T F_\epsilon, \quad \Xi_{\epsilon,\sigma}^{2,4} \triangleq \left(I_N \otimes P_{2\epsilon,\sigma}\right)\hat{B}_{d\epsilon} \\ \bar{\Xi}_{\epsilon,\sigma}^{1,2} &\triangleq \left(I_N \otimes P_{1\epsilon,\sigma}\right)\hat{C}_\epsilon, \quad \Xi_{\epsilon,\sigma}^{2,3} \triangleq \left(I_N \otimes P_{2\epsilon,\sigma}\right)\hat{L}_\sigma \hat{E}_\epsilon \\ \bar{\Xi}_{\epsilon,\sigma}^{1,3} &\triangleq \left(I_N \otimes P_{1\epsilon,\sigma}\right)\hat{E}_\epsilon, \quad \Phi \triangleq \mathrm{diag}\left\{\varrho_1^2, \varrho_2^2, \ldots, \varrho_n^2\right\} \\ \bar{\Xi}_{\epsilon,\sigma}^{2,2} &\triangleq 2\left(I_N \otimes P_{2\epsilon,\sigma} A_{d\epsilon}\right) + 2\left(I_N \otimes P_{2\epsilon,\sigma}\right)\hat{L}_\sigma \hat{C}_\epsilon + \bar{P}_{2q,\delta} \\ \hat{\mathcal{D}}_{\epsilon,\sigma} &\triangleq -\sum_{k=1}^{\varkappa} \frac{\pi^2}{4 l_k^2}\left(P_{1\epsilon,\sigma} D_k + D_k^T P_{1\epsilon,\sigma}\right) \\ \bar{P}_{1q,\delta} &\triangleq \sum_{(q,\delta)\in\mathcal{M}\times\mathcal{W}} \rho_{(\epsilon,\sigma)(q,\delta)}\left(I_N \otimes P_{1q,\delta}\right) \\ \bar{P}_{2q,\delta} &\triangleq \sum_{(q,\delta)\in\mathcal{M}\times\mathcal{W}} \rho_{(\epsilon,\sigma)(q,\delta)}\left(I_N \otimes P_{2q,\delta}\right)\end{aligned}$$

then the bipartite synchronization of network dynamics (2) and (6) under the composite controller (13) is achieved subject to the predescribed H_∞ performance index γ.

Proof: Consider the following Lyapunov candidate function:

$$\begin{aligned}&V(e_{t,x}, e_{\bar{\eta},t,x}, \hbar(t), t) \\ &= \int_\Omega e_{t,x}^T \left(I_N \otimes P_{1\epsilon,\sigma}\right) e_{t,x} dx \\ &\quad + \int_\Omega e_{\bar{\eta},t,x}^T \left(I_N \otimes P_{2\epsilon,\sigma}\right) e_{\bar{\eta},t,x} dx. \qquad (22)\end{aligned}$$

The weak infinitesimal operator $\mathfrak{L}$ associated with the Markov process is given by

$$\begin{aligned}&\mathfrak{L}[V(e_{t,x}, e_{\tilde{\eta},t,x}, \hbar_t, t)]\\ &\triangleq \lim_{\nabla\to 0^+} \frac{1}{\nabla}\{E\{V(e_{t+\nabla,x}, e_{\tilde{\eta},t+\nabla,x}, \hbar_{t+\nabla}, t+\nabla)|_{e_{t,x},e_{\tilde{\eta},t,x},\hbar_t}\}\\ &\qquad - V(e_{t,x}, e_{\tilde{\eta},t,x}, \hbar_t, t)\}. \qquad (23)\end{aligned}$$

For convenience, let $\mathfrak{L}V_{(t)} \triangleq \mathfrak{L}[V(e_{t,x}, e_{\tilde{\eta},t,x}, \hbar_t, t)]$. According to (23), one has

$$\begin{aligned}\mathfrak{L}V_{(t)} = &\int_\Omega 2e_{t,x}^T\left(I_N\otimes P_{1\epsilon,\sigma}\right)\frac{\partial e_{t,x}}{\partial t}dx\\ &+\int_\Omega 2e_{\tilde{\eta},t,x}^T\left(I_N\otimes P_{2\epsilon,\sigma}\right)\frac{\partial e_{\tilde{\eta},t,x}}{\partial t}dx\\ &+\int_\Omega e_{t,x}^T\bar{P}_{1q,\delta}e_{t,x}dx+\int_\Omega e_{t,x}^T\bar{P}_{2q,\delta}e_{t,x}dx. \qquad (24)\end{aligned}$$

For the composite system (16), with or without disturbances $\Gamma_{t,x}$, stability criteria and the H_∞ performance analysis are presented as follows.

Step 1: Suppose that $\Gamma_{t,x}\equiv 0$. Then, we have

$$\begin{aligned}&\int_\Omega 2e_{t,x}^T\left(I_N\otimes P_{1\epsilon,\sigma}\right)\frac{\partial e_{t,x}}{\partial t}dx\\ &=\int_\Omega 2e_{t,x}^T\left(I_N\otimes P_{1\epsilon,\sigma}\right)(\hat{D}_k\Delta e_{t,,x}+\hat{A}_\epsilon e_{t,x}\\ &\quad+\hat{B}_\epsilon f(e_{t,x})+\hat{C}_\epsilon e_{\tilde{\eta},t,x})dx,\\ &\int_\Omega 2e_{\tilde{\eta},t,x}^T\left(I_N\otimes P_{2\epsilon,\sigma}\right)\frac{\partial e_{\tilde{\eta},t,x}}{\partial t}dx\\ &=\int_\Omega 2e_{\tilde{\eta},t,x}^T\left(I_N\otimes P_{2\epsilon,\sigma}\right)(\hat{A}_{d\epsilon}+\hat{L}_\sigma\hat{C}_\epsilon)e_{\tilde{\eta},t,x}dx. \qquad (25)\end{aligned}$$

By invoking Lemma 1 in [25], it yields

$$\int_\Omega 2e_{t,x}^T(I_N\otimes P_{1\epsilon,\sigma}D_k)\Delta e_{t,x}dx\le\int_\Omega e_{t,x}^T(I_N\otimes\hat{\mathcal{D}}_{\epsilon,\sigma})e_{t,x}dx \qquad (26)$$

where $\hat{\mathcal{D}}_{\epsilon,\sigma}\triangleq-\sum_{k=1}^{\varkappa}(\pi^2)/(4l_k^2)(P_{1\epsilon,\sigma}D_k+D_k^TP_{1\epsilon,\sigma})$.

Applying the Assumption 2 in [25], it follows that:

$$\begin{aligned}&2e_{t,x}^T(I_N\otimes P_{1\epsilon,\sigma}\hat{B}_\epsilon)f(e_{t,x})\\ &\quad\le e_{t,x}^T[I_N\otimes\left(P_{1\epsilon,\sigma}\hat{B}_\epsilon\hat{B}_\epsilon^TP_{1\epsilon,\sigma}+\Phi\right)]e_{t,x} \qquad (27)\end{aligned}$$

with $\Phi\triangleq\text{diag}\{\varrho_1^2,\varrho_2^2,\ldots,\varrho_n^2\}$, where ϱ_ι is known constant for $\iota=1,2,\ldots,n$.

Integrating (24)–(27), one obtains

$$\mathfrak{L}V_{(t)}\le\int_\Omega\zeta_{t,x}^T\bar{\Xi}_{\epsilon,\sigma}\zeta_{t,x}dx \qquad (28)$$

with

$$\bar{\Xi}_{\epsilon,\sigma}\triangleq\begin{bmatrix}\bar{\Xi}_{\epsilon,\sigma}^{1,1} & \bar{\Xi}_{\epsilon,\sigma}^{1,2}\\ * & \bar{\Xi}_{\epsilon,\sigma}^{2,2}\end{bmatrix},\quad \zeta_{t,x}\triangleq\begin{bmatrix}e_{t,x}\\ e_{\tilde{\eta},t,x}\end{bmatrix}.$$

According to (20), one can see that $\mathfrak{L}V_{(t)}<0$ holds.

Moreover, denoting $\hat{\lambda}\triangleq\{\hat{\lambda}_{\min}(-\bar{\Xi}_{\epsilon,\sigma}),\epsilon\in\mathcal{M},\sigma\in\mathcal{W}\}$, one has

$$\mathcal{E}\{\mathfrak{L}V_{(t)}\}<-\hat{\lambda}\mathcal{E}\left\{\int_\Omega\zeta_{t,x}^T\zeta_{t,x}dx\right\}<-\hat{\lambda}\mathcal{E}\{\|\zeta_{t,x}\|^2\}. \qquad (29)$$

According to Dynkin's formula, we have

$$\mathcal{E}\{V_{(t_f)}-V_{(0)}\}=\int_0^{t_f}\mathcal{E}\{\mathfrak{L}V_{(t)}\}dt. \qquad (30)$$

From (29) and (30), one can derive that

$$\begin{aligned}\int_0^{t_f}\mathcal{E}\{\mathfrak{L}V_{(t)}\}dt&=\mathcal{E}\{V_{(t_f)}-V_{(0)}\}\\ &<-\hat{\lambda}\mathcal{E}\left\{\int_0^{t_f}\|\zeta_{t,x}\|^2dt\right\}. \qquad (31)\end{aligned}$$

Then, one has

$$\lim_{t_f\to\infty}\mathcal{E}\left\{\int_0^{t_f}\|\zeta_{t,x}\|^2dt\right\}<\frac{\mathcal{E}\{V_{(0)}\}}{\hat{\lambda}}<\infty.$$

In view of Definition 1, the composite system (16) is stochastically stable.

Step 2: For zero initial conditions and disturbances $\Gamma_{t,x}\neq 0$, consider the following H_∞ performance index expressed as:

$$\mathcal{J}=\mathcal{E}\left\{\int_0^{t_f}\int_\Omega\left[y_{t,x}^Ty_{t,x}-\gamma^2\Gamma_{t,x}^T\Gamma_{t,x}\right]dxdt\right\}. \qquad (32)$$

Based on (30) and (32) under zero initial conditions, one has

$$\begin{aligned}\mathcal{J}&=\mathcal{E}\left\{\int_0^{t_f}\int_\Omega\left[y_{t,x}^Ty_{t,x}-\gamma^2\Gamma_{t,x}^T\Gamma_{t,x}\right]dxdt\right\}\\ &\quad+\mathcal{E}\left\{\int_0^{t_f}\mathfrak{L}V_{(t)}dt\right\}-\mathcal{E}\left\{V_{(t_f)}-V_{(0)}\right\}\\ &\le\mathcal{E}\left\{\int_0^{t_f}\int_\Omega\left[y_{t,x}^Ty_{t,x}-\gamma^2\Gamma_{t,x}^T\Gamma_{t,x}\right]dxdt\right\}\\ &\quad+\mathcal{E}\left\{\int_0^{t_f}\mathfrak{L}V_{(t)}dt\right\}. \qquad (33)\end{aligned}$$

Combining (28) with (33), we can derive

$$\begin{aligned}\mathcal{J}=\mathcal{E}\Big\{\int_0^{t_f}\int_\Omega&[e_{t,x}^T\left(I_N\otimes F_\epsilon^TF_\epsilon\right)e_{t,x}-\gamma^2\Gamma_{t,x}^T\Gamma_{t,x}\\ &-e_{t,x}^T\left(I_N\otimes P_{1\epsilon,\sigma}\right)\hat{E}_\epsilon w_{t,x}+e_{\tilde{\eta},t,x}^T\left(I_N\otimes P_{2\epsilon,\sigma}\right)\hat{B}_{d\epsilon}\omega_{t,x}\\ &+e_{\tilde{\eta},t,x}^T\left(I_N\otimes P_{2\epsilon,\sigma}\right)\hat{L}_\sigma\hat{E}_\epsilon w_{t,x}+e_{t,x}^T\bar{\Xi}_{\epsilon,\sigma}e_{t,x}]dxdt\Big\}\\ \le\mathcal{E}\left\{\int_0^{t_f}\int_\Omega\check{\zeta}_{t,x}^T\Xi_{\epsilon,\sigma}\check{\zeta}_{t,x}dxdt\right\}& \qquad (34)\end{aligned}$$

where

$$\check{\zeta}_{t,x}\triangleq\left[\,e_{t,x}^T\;e_{\tilde{\eta},t,x}^T\;\Gamma_{t,x}^T\,\right]^T.$$

From (21), it can be deduced that $\mathcal{J}<0$.

Hence, when $t_f\to\infty$, it can be concluded that

$$\mathcal{E}\left\{\int_0^\infty\int_\Omega\left[y_{t,x}^Ty_{t,x}-\gamma^2\Gamma_{t,x}^T\Gamma_{t,x}\right]dxdt\right\}<0. \qquad (35)$$

According to Definition 2 in [25], the bipartite synchronization of network dynamics (2) and (6) is achieved subject to the desired H_∞ performance index γ. The proof is completed.

B. Controller Design

Theorem 2: If there exist positive definite diagonal matrices $X_{1\epsilon,\sigma}\in\mathbb{R}^{n\times n}$ and $P_{2\epsilon,\sigma}\in\mathbb{R}^{n_\eta\times n_\eta}$ such that the following conditions hold for all $\epsilon\in\mathcal{M}$ and $\sigma\in\mathcal{W}$

$$I_N\otimes(\varepsilon_{1\epsilon}D_k\mathbb{N}_{1\sigma}+\varepsilon_{1\epsilon}\mathbb{N}_{1\sigma}D_k^T)\quad>0 \qquad (36)$$

$$\begin{bmatrix} \Lambda^{1,1}_{\epsilon,\sigma} & \Lambda^{1,2}_{\epsilon,\sigma} & \Lambda^{1,3}_{\epsilon,\sigma} & 0 & \Lambda^{1,5}_{\epsilon,\sigma} & \Lambda^{1,6}_{\epsilon,\sigma} & \Lambda^{1,7}_{\epsilon,\sigma} \\ * & \Lambda^{2,2}_{\epsilon,\sigma} & \Lambda^{2,3}_{\epsilon,\sigma} & \Lambda^{2,4}_{\epsilon,\sigma} & 0 & 0 & 0 \\ * & * & -\gamma^2 I_{n_w} & 0 & 0 & 0 & 0 \\ * & * & * & -\gamma^2 I_{n_\omega} & 0 & 0 & 0 \\ * & * & * & * & \Lambda^{5,5}_{\epsilon,\sigma} & 0 & 0 \\ * & * & * & * & * & \Lambda^{6,6}_{\epsilon,\sigma} & 0 \\ * & * & * & * & * & * & \Lambda^{7,7}_{q,\delta} \end{bmatrix} < 0 \quad (37)$$

with

$$\begin{aligned}
\Lambda^{1,1}_{\epsilon,\sigma} &\triangleq I_N \otimes \left(-\sum_{k=1}^{\varkappa} \frac{\varepsilon_{1\epsilon}\pi^2}{4l_k^2} \left(D_k \mathbb{N}_{1\sigma} + \mathbb{N}_{1\sigma} D_k^T \right) + B_\epsilon B_\epsilon^T \right) \\
&\quad + \rho_{(\epsilon,\sigma)(q,\delta)} \varepsilon_{1\epsilon} (I_N \otimes \mathbb{N}_{1\sigma}) - 2\varepsilon_{1\epsilon} (I_N \otimes A_\epsilon \mathbb{N}_{1\sigma}) \\
&\quad - 2c\varepsilon_{1\epsilon} \left(\check{\mathcal{V}}_\epsilon \otimes \mathbb{N}_{1\sigma} \right) + 2 (I_N \otimes C_\epsilon) \breve{\mu} \check{\mathcal{K}}_{\epsilon,\sigma} \\
\Lambda^{2,2}_{\epsilon,\sigma} &\triangleq 2\varepsilon_{2\epsilon} (I_N \otimes \mathbb{N}_{2\sigma} A_{d\epsilon}) + 2\check{L}_{\epsilon,\sigma} (\bar{\mu} \otimes C_\epsilon C_{d\epsilon}) \\
&\quad + \sum_{(q,\delta)\in\mathcal{M}\times\mathcal{W}} \rho_{(\epsilon,\sigma)(q,\delta)} \varepsilon_{2q} (I_N \otimes \mathbb{N}_{2\delta}) \\
\Lambda^{1,2}_{\epsilon,\sigma} &\triangleq \bar{\mu} \otimes C_\epsilon C_{d\epsilon}, \Lambda^{2,4}_{\epsilon,\sigma} \triangleq \varepsilon_{2\epsilon} (I_N \otimes \mathbb{N}_{2\sigma}) \hat{B}_{d\epsilon} \\
\Lambda^{1,3}_{\epsilon,\sigma} &\triangleq \hat{E}_\epsilon, \Lambda^{2,3}_{\epsilon,\sigma} \triangleq \check{L}_{\epsilon,\sigma} \hat{E}_\epsilon, \Lambda^{5,5}_{\epsilon,\sigma} \triangleq -I_N \otimes I_n \\
\Lambda^{1,5}_{\epsilon,\sigma} &\triangleq \varepsilon_{1\epsilon} \left(I_N \otimes \mathbb{N}_{1\sigma} F_\epsilon^T \right), \Lambda^{1,6}_{\epsilon,\sigma} \triangleq \varepsilon_{1\epsilon} \left(I_N \otimes \sqrt{\Phi} \mathbb{N}_{1\sigma} \right) \\
\Lambda^{1,7}_{\epsilon,\sigma} &\triangleq \varepsilon_{1\epsilon} \left[\Theta^{1N}_{\epsilon,\sigma} \cdots \Theta^{qN}_{\epsilon,\sigma} \cdots \Theta^{GN}_{\epsilon,\sigma} \right], \Lambda^{6,6}_{\epsilon,\sigma} \triangleq -I_N \otimes I_n \\
\Lambda^{7,7}_{q,\delta} &\triangleq \mathrm{diag}\left\{ -\Pi_{1N}, \ldots, -\Pi_{qN}, \ldots, -\Pi_{GN} \right\} \\
\Theta^{1N}_{\epsilon,\sigma} &\triangleq I_N \otimes \left[\sqrt{\rho_{(\epsilon,\sigma)(1,1)}} \mathbb{N}_{1\sigma} \right. \\
&\qquad \left. \cdots \sqrt{\rho_{(\epsilon,\sigma)(1,\sigma)}} \mathbb{N}_{1\sigma} \cdots \sqrt{\rho_{(\epsilon,\sigma)(1,N)}} \mathbb{N}_{1\sigma} \right] \\
\Theta^{qN}_{\epsilon,\sigma} &\triangleq I_N \otimes \left[\sqrt{\rho_{(\epsilon,\sigma)(q,1)}} \mathbb{N}_{1\sigma} \right. \\
&\qquad \left. \cdots \sqrt{\rho_{(\epsilon,\sigma)(q,\sigma)}} \mathbb{N}_{1\sigma} \cdots \sqrt{\rho_{(\epsilon,\sigma)(q,N)}} \mathbb{N}_{1\sigma} \right] \\
\Theta^{GN}_{\epsilon,\sigma} &\triangleq I_N \otimes \left[\sqrt{\rho_{(\epsilon,\sigma)(G,1)}} \mathbb{N}_{1\sigma} \right. \\
&\qquad \left. \cdots \sqrt{\rho_{(\epsilon,\sigma)(G,\sigma)}} \mathbb{N}_{1\sigma} \cdots \sqrt{\rho_{(\epsilon,\sigma)(G,N)}} \mathbb{N}_{1\sigma} \right] \\
\Pi_{1N} &\triangleq \varepsilon_{1\epsilon} I_N \otimes \mathrm{diag}\left\{ \mathbb{N}_{11}, \ldots, \mathbb{N}_{1\sigma}, \ldots, \mathbb{N}_{1N} \right\} \\
\Pi_{qN} &\triangleq \varepsilon_{1q} I_N \otimes \mathrm{diag}\left\{ \mathbb{N}_{11}, \ldots, \mathbb{N}_{1\sigma}, \ldots, \mathbb{N}_{1N} \right\} \\
\Pi_{GN} &\triangleq \varepsilon_{1G} I_N \otimes \mathrm{diag}\left\{ \mathbb{N}_{11}, \ldots, \mathbb{N}_{1\sigma}, \ldots, \mathbb{N}_{1N} \right\}
\end{aligned}$$

then the composite system (16) is globally asymptotically stable subject to the presented H_∞ performance index γ, in which the desired controller gain and the observer gain, for $\epsilon \in \mathcal{M}$, $\sigma \in \mathcal{W}$, are described by

$$\begin{aligned} \mathcal{K}_\sigma &= \check{\mathcal{K}}_{\epsilon,\sigma} (I_N \otimes X^{-1}_{1\epsilon,\sigma}) \\ \hat{L}_\sigma &= (I_N \otimes P^{-1}_{2\epsilon,\sigma}) \check{L}_{\epsilon,\sigma}. \end{aligned} \quad (38)$$

Proof: First, let $P_{1\epsilon,\sigma} = X^{-1}_{1\epsilon,\sigma}$. By pre- and postmultiplying (19) and (21) by $X_{1\epsilon,\sigma}$ and $\mathrm{diag}\{I_N \otimes X_{1\epsilon,\sigma}, I_N \otimes I_n, I_N \otimes I_n, I_N \otimes I_n\}$, respectively. Then, one gets

$$I_N \otimes (D_k X_{1\epsilon,\sigma} + X_{1\epsilon,\sigma} D_k^T) > 0 \quad (39)$$

$$\Upsilon_{\epsilon,\sigma} \triangleq \begin{bmatrix} \Upsilon^{1,1}_{\epsilon,\sigma} & \Upsilon^{1,2}_{\epsilon,\sigma} & \Upsilon^{1,3}_{\epsilon,\sigma} & 0 \\ * & \Xi^{2,2}_{\epsilon,\sigma} & \Xi^{2,3}_{\epsilon,\sigma} & \Xi^{2,4}_{\epsilon,\sigma} \\ * & * & -\gamma^2 I_{n_w} & 0 \\ * & * & * & -\gamma^2 I_{n_\omega} \end{bmatrix} < 0 \quad (40)$$

with

$$\begin{aligned}
\Upsilon^{1,1}_{\epsilon,\sigma} &\triangleq I_N \otimes \left(-\sum_{k=1}^{\varkappa} \frac{\pi^2}{4l_k^2} \left(D_k X_{1\epsilon,\sigma} + X_{1\epsilon,\sigma} D_k^T \right) + \check{\Phi} \right) \\
&\quad + \sum_{(q,\delta)\in\mathcal{M}\times\mathcal{W}} \rho_{(\epsilon,\sigma)(q,\delta)} \left(I_N \otimes X_{1\epsilon,\sigma} X^{-1}_{1q,\delta} X_{1\epsilon,\sigma} \right) \\
&\quad - 2 \left(I_N \otimes \left(A_\epsilon X_{1\epsilon,\sigma} \right) + I_N \otimes X_{1\epsilon,\sigma} F_\epsilon^T F_\epsilon X_{1\epsilon,\sigma} \right. \\
&\quad \left. + c \left(\check{\mathcal{V}}_\epsilon \otimes X_{1\epsilon,\sigma} \right) - (I_N \otimes C_\epsilon) \breve{\mu} \mathcal{K}_\sigma \left(I_N \otimes X_{1\epsilon,\sigma} \right) \right) \\
\Upsilon^{1,2}_{\epsilon,\sigma} &\triangleq \bar{\mu} \otimes C_\epsilon C_{d\epsilon}, \quad \Upsilon^{1,3}_{\epsilon,\sigma} \triangleq \hat{E}_\epsilon, \check{\Phi} \triangleq B_\epsilon B_\epsilon^T + X_{1\epsilon,\sigma} \Phi X_{1\epsilon,\sigma}.
\end{aligned}$$

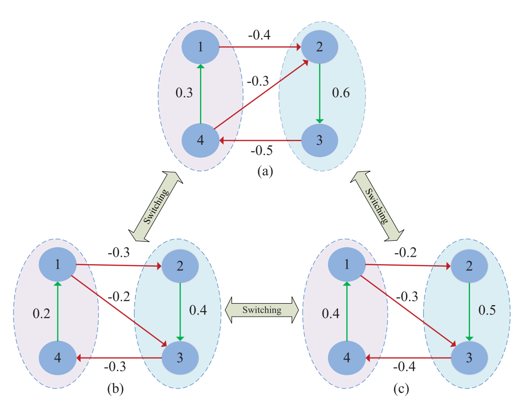

Fig. 2. Switching topologies $\mathfrak{R}_1$, $\mathfrak{R}_2$ and $\mathfrak{R}_3$. (a) Signed graph $\mathfrak{R}_1$. (b) Signed graph $\mathfrak{R}_2$. (c) Signed graph $\mathfrak{R}_3$.

After that, applying the Schur complement to (40). With respect to inequality (37), we have

$$\begin{aligned} \check{\mathcal{K}}_{\epsilon,\sigma} &\triangleq \mathcal{K}_\sigma (I_N \otimes X_{1\epsilon,\sigma}) \\ \check{L}_{\epsilon,\sigma} &\triangleq (I_N \otimes P_{2\epsilon,\sigma}) \hat{L}_\sigma. \end{aligned} \quad (41)$$

Define $X_{1\epsilon,\sigma} = \varepsilon_{1\epsilon} \Bbbk_{1\epsilon} \mathbb{N}_{1\sigma}$ and $P_{2\epsilon,\sigma} = \varepsilon_{2\epsilon} \Bbbk_{2\epsilon} \mathbb{N}_{2\sigma}$, for each $\epsilon \in \mathcal{M}$ and $\sigma \in \mathcal{W}$, where $\Bbbk_{1\epsilon}$ and $\Bbbk_{2\epsilon}$ are invertible identity matrices. Thus, it yields that $X_{1\epsilon,\sigma} = \varepsilon_{1\epsilon} \mathbb{N}_{1\sigma}$ and $P_{2\epsilon,\sigma} = \varepsilon_{2\epsilon} \mathbb{N}_{2\sigma}$.

Then, one derives the following conditions:

$$\begin{aligned} \check{\mathcal{K}}_{\epsilon,\sigma} &\triangleq \varepsilon_{1\epsilon} \mathcal{K}_\sigma (I_N \otimes \mathbb{N}_{1\sigma}) \\ \check{L}_{\epsilon,\sigma} &\triangleq \varepsilon_{2\epsilon} (I_N \otimes \mathbb{N}_{2\sigma}) \hat{L}_\sigma. \end{aligned} \quad (42)$$

Finally, by integrating (39)–(42), inequalities (36) and (37) can be obtained. This completes the proof.

IV. Performance Analysis

In this section, the effectiveness of the proposed composite antidisturbance H_∞ control method is illustrated. Consider the CCNNs with switched topologies and RDTs, consisting of four nodes (i.e., $N = 4$), where each node contains two neurons (namely, $n = 2$). As shown in Fig. 2, the corresponding switched topologies $\mathfrak{R}_1$, $\mathfrak{R}_2$ and $\mathfrak{R}_3$, are defined, in which the overall set of nodes is partitioned into two subsets: $\mathfrak{I}_1 = \{1, 4\}$ and $\mathfrak{I}_2 = \{2, 3\}$. The Laplacian matrices $\mathcal{V}_1, \mathcal{V}_2$ and $\mathcal{V}_3$ are defined by

$$\mathcal{V}_1 = \begin{bmatrix} 0.3 & 0 & 0 & -0.3 \\ 0.4 & 0.7 & 0 & 0.3 \\ 0 & -0.6 & 0.6 & 0 \\ 0 & 0 & 0.5 & 0.5 \end{bmatrix}$$

$$\mathcal{V}_2 = \begin{bmatrix} 0.2 & 0 & 0 & -0.2 \\ 0.3 & 0.3 & 0 & 0 \\ 0.2 & -0.4 & 0.6 & 0 \\ 0 & 0 & 0.3 & 0.3 \end{bmatrix}$$

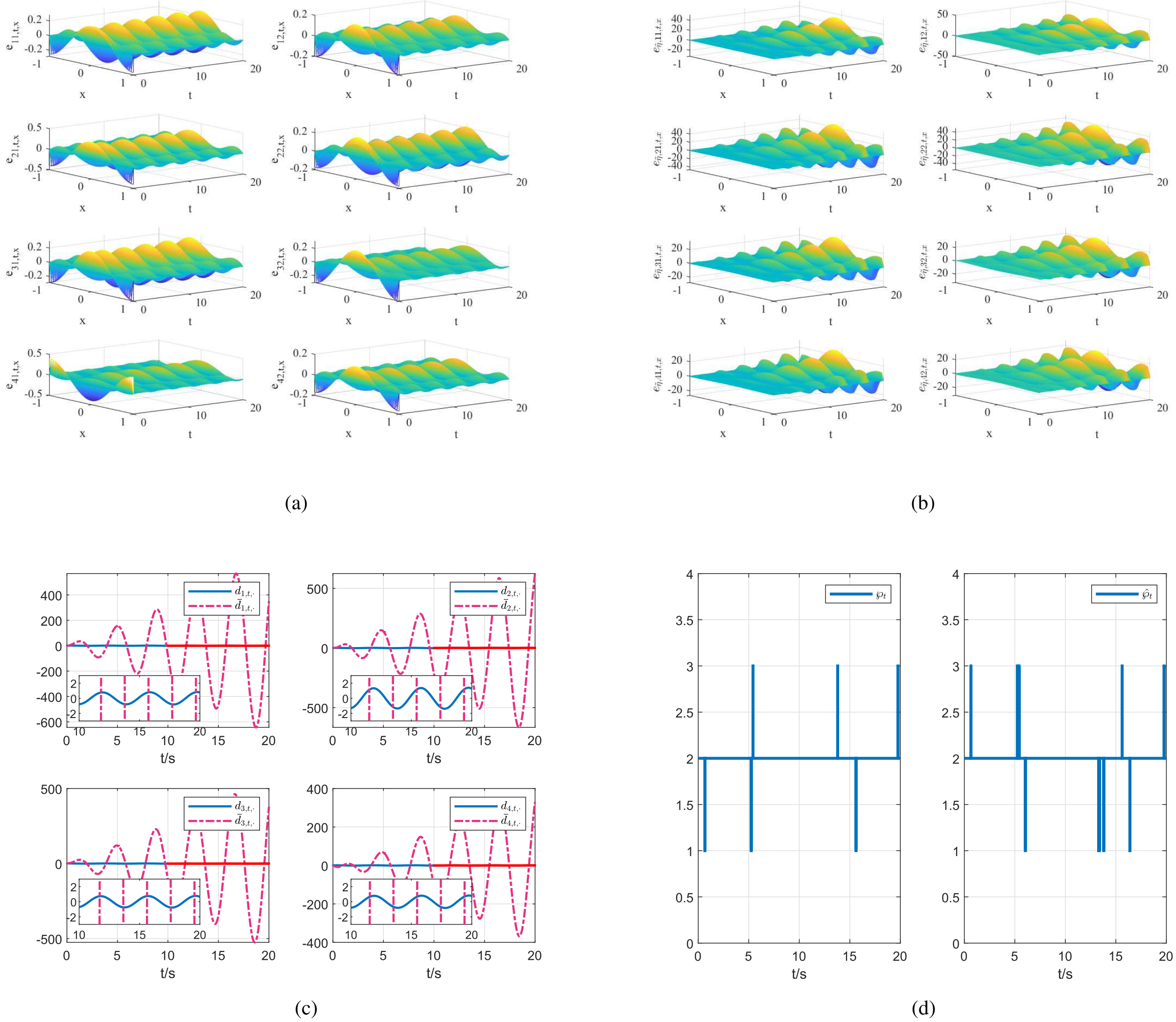

Fig. 3. Spatial responses without control input. (a) Responses of BSES (14). (b) Responses of estimation error system (15). (c) Disturbance $d_{i,t,\cdot}$ and its estimation $\bar{d}_{i,t,\cdot}$, for $i = 1, 2, 3, 4$. (d) Hidden mode sequence $\wp_t$ of the composite system (16) and the observer mode sequence $\hat{\wp}_t$ of the controller (13).

$$\mathcal{V}_3 = \begin{bmatrix} 0.4 & 0 & 0 & -0.4 \\ 0.2 & 0.2 & 0 & 0 \\ 0.3 & -0.5 & 0.8 & 0 \\ 0 & 0 & 0.4 & 0.4 \end{bmatrix}.$$

The gauge transformation matrix is given by $\bar{\mu} \triangleq \text{diag}\{-1, 1, 1, -1\}$. Moreover, suppose that Π_α^σ is the detection probability matrix, Π_β and Π_λ^ϵ denote TR matrices corresponding to $\wp_t$ and $\hat{\wp}_t$, respectively, which are assumed to be given by

$$\Pi_\alpha^\sigma = \begin{bmatrix} 0.4 & 0.21 & 0.39 \\ 0.2 & 0.5 & 0.3 \\ 0.4 & 0.14 & 0.46 \end{bmatrix}$$

$$\Pi_\beta = \begin{bmatrix} -0.401 & 0.301 & 0.1 \\ 0.5 & -0.9 & 0.4 \\ 0.3 & 0.21 & -0.51 \end{bmatrix}$$

$$\Pi_\lambda^\epsilon = \begin{bmatrix} -0.31 & 0.11 & 0.2 \\ 0.4 & -0.501 & 0.101 \\ 0.201 & 0.7 & -0.901 \end{bmatrix}$$

with $\alpha = \beta = \lambda = 1, 2, 3$. Based on (10) and (11), the final TR matrix can be computed. Let $i = 1, 2, 3, 4$, $\varkappa = 1$, and $(t, x) \in [0, 20] \times [-1, 1]$. Define the following system parameters: the coupling strength $c = 1$, the external disturbances $w_{t,x} = 0.5\cos(\pi x)/(1 + t^2)$ and $\omega_{t,x} = 0.5\cos(\pi x)\exp(-0.02t)$, the activation function $f(\vartheta_{i,t,x}) = \tanh(\vartheta_{i,t,x})$ with the bound being $\varrho_1 = \varrho_2 = 1$, and the H_∞ performance index $\gamma = 1.2$. In addition, system parameters of each node with two modes are listed below

$$D_1 = \text{diag}\{0.16, 0.16\}, \quad C_1 = \text{diag}\{-0.9, 0.56\}$$
$$C_2 = \text{diag}\{-0.85, 0.5\}, \quad C_3 = \text{diag}\{-0.72, 0.5\}$$
$$A_1 = \text{diag}\{1, 0.8\}, \quad A_2 = \text{diag}\{1.1, 1.0\}, \quad A_3 = \text{diag}\{0.7, 0.5\}$$
$$B_1 = \begin{bmatrix} 0.24 & -0.16 \\ 0.16 & 0.32 \end{bmatrix}, \quad B_2 = \begin{bmatrix} 0.4 & 0.24 \\ 0.5 & 0.6 \end{bmatrix}$$
$$B_3 = \begin{bmatrix} 0.3 & -0.2 \\ -0.3 & 0.5 \end{bmatrix}$$
$$E_{i1} = \begin{bmatrix} 0.08 & 0.16 \end{bmatrix}^T, \quad E_{i2} = \begin{bmatrix} 0.11 & 0.08 \end{bmatrix}^T$$

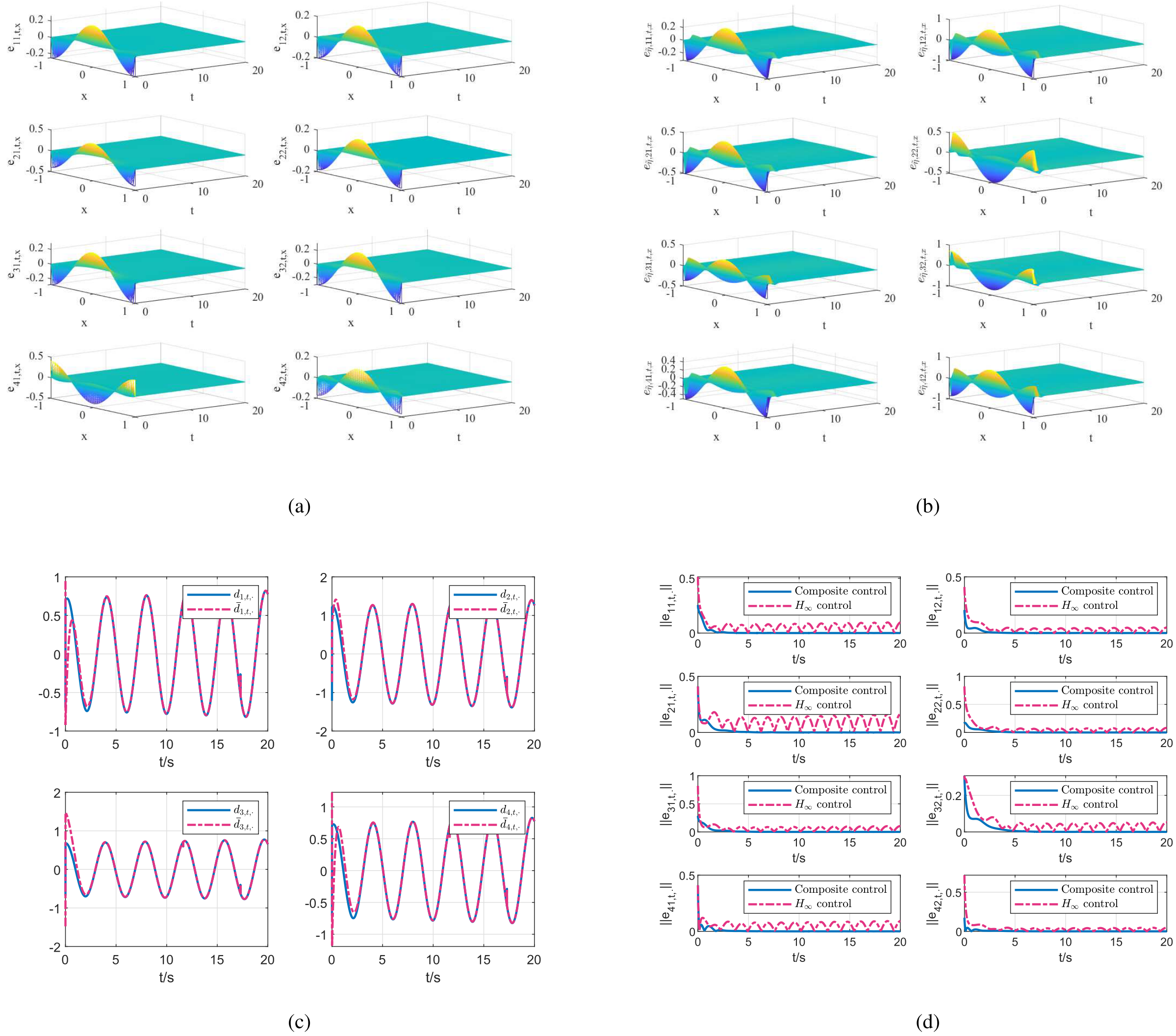

Fig. 4. Spatial responses with control input. (a) Responses of BSES (14). (b) Responses of estimation error system (15). (c) Disturbance $d_{i,t,\cdot}$ and its estimation $\bar{d}_{i,t,\cdot}$, for $i = 1, 2, 3, 4$. (d) Error states $\|e_{ij,t,\cdot}\|$, for $i = 1, 2, 3, 4$, $j = 1, 2$.

$$F_3 = \begin{bmatrix} 0.12 & 0.3 \\ 0 & 0.16 \end{bmatrix}$$
$$F_1 = \begin{bmatrix} 0.24 & 0.16 \\ 0 & 0.3 \end{bmatrix}, \quad F_2 = \begin{bmatrix} 0.4 & 0.3 \\ 0 & 0.2 \end{bmatrix}$$
$$E_{i3} = \begin{bmatrix} 0.08 & 0.12 \end{bmatrix}^T.$$

Define $\Upsilon_x = \cos(\pi x)$. The initial conditions are assumed to be

$$\phi_{1,x} = \begin{bmatrix} 0.5\Upsilon_x & 0.5\Upsilon_x \end{bmatrix}^T, \quad \phi_{2,x} = \begin{bmatrix} 0.6\Upsilon_x & 0.68\Upsilon_x \end{bmatrix}^T$$
$$\phi_{3,x} = \begin{bmatrix} 0.58\Upsilon_x & 0.6\Upsilon_x \end{bmatrix}^T, \quad \phi_{4,x} = \begin{bmatrix} -0.5\Upsilon_x & 0.47\Upsilon_x \end{bmatrix}^T$$

and initial conditions of the isolated node dynamic (6) are listed as

$$\breve{\phi}_{1,x} = \begin{bmatrix} 0.25\Upsilon_x & 0.3\Upsilon_x \end{bmatrix}^T, \quad \breve{\phi}_{2,x} = \begin{bmatrix} 0.2\Upsilon_x & 0.5\Upsilon_x \end{bmatrix}^T$$
$$\breve{\phi}_{3,x} = \begin{bmatrix} 0.3\Upsilon_x & 0.3\Upsilon_x \end{bmatrix}^T, \quad \breve{\phi}_{4,x} = \begin{bmatrix} -0.1\Upsilon_x & 0.3\Upsilon_x \end{bmatrix}^T.$$

Meanwhile, exogenous system parameters of each node with two modes are set as

$$A_{d1} = \begin{bmatrix} 0 & 1.6 \\ -1.6 & 0 \end{bmatrix}, \quad A_{d2} = \begin{bmatrix} 0 & 2.4 \\ -2.4 & 0 \end{bmatrix}$$
$$A_{d3} = \begin{bmatrix} 0 & 1.7 \\ -1.7 & 0 \end{bmatrix}$$
$$B_{di1} = \begin{bmatrix} 0.06 & 0.08 \end{bmatrix}^T, \quad C_{d2} = \begin{bmatrix} 1.6 & 1.2 \end{bmatrix}$$
$$C_{d3} = \begin{bmatrix} 1.3 & 1.6 \end{bmatrix}$$
$$C_{d1} = \begin{bmatrix} 1.2 & 1.7 \end{bmatrix}, \quad B_{di2} = \begin{bmatrix} 0.11 & 0.08 \end{bmatrix}^T$$
$$B_{di3} = \begin{bmatrix} 0.04 & 0.08 \end{bmatrix}^T.$$

The spatial responses of the BSES (14) and the estimation error system (15) without the control input are shown in Fig. 3(a) and (b). It is evident from the two figures that systems exhibit instability. As one can see from Fig. 3(c), it is obvious that the unknown disturbance $d_{i,t,x}$ ($i = 1, 2, 3, 4$) can not be estimated. Fig. 3(d) plots the switching sequence of system

TABLE I
COMPARISON OF $\gamma_{\min}$ UNDER DIFFERENT VALUES OF THE SYSTEM MATRIX D_1

D_1	$\begin{bmatrix}0.12 & 0\\ 0 & 0.12\end{bmatrix}$	$\begin{bmatrix}0.13 & 0\\ 0 & 0.13\end{bmatrix}$	$\begin{bmatrix}0.14 & 0\\ 0 & 0.14\end{bmatrix}$	$\begin{bmatrix}0.15 & 0\\ 0 & 0.15\end{bmatrix}$
Th. 2	0.4992	0.3988	0.3734	0.3627
H_∞	0.5111	0.4148	0.3858	0.3663

and controller. In view of the proposed CDRC scheme, state-feedback controller gains are computed as follows:

$$
\begin{aligned}
K_{1,1} &= \begin{bmatrix}-3.7249 & 2.1565\end{bmatrix}, & K_{1,2} &= \begin{bmatrix}-3.6188 & 2.1504\end{bmatrix}\\
K_{1,3} &= \begin{bmatrix}-3.2817 & 2.0217\end{bmatrix}, & K_{2,1} &= \begin{bmatrix}3.3741 & -2.2724\end{bmatrix}\\
K_{2,2} &= \begin{bmatrix}3.2319 & -2.2192\end{bmatrix}, & K_{2,3} &= \begin{bmatrix}2.9312 & -2.0668\end{bmatrix}\\
K_{3,1} &= \begin{bmatrix}2.8459 & -1.8188\end{bmatrix}, & K_{3,2} &= \begin{bmatrix}2.7181 & -1.7758\end{bmatrix}\\
K_{3,3} &= \begin{bmatrix}2.4400 & -1.6428\end{bmatrix}, & K_{4,1} &= \begin{bmatrix}-3.5066 & 2.1700\end{bmatrix}\\
K_{4,2} &= \begin{bmatrix}-3.3504 & 2.1196\end{bmatrix}, & K_{4,3} &= \begin{bmatrix}-3.0840 & 2.2540\end{bmatrix}\\
L_{1,1} &= \mathrm{diag}\{-0.6150, 2.6899\}\\
L_{1,2} &= \mathrm{diag}\{-0.6129, 2.7057\}\\
L_{1,3} &= \mathrm{diag}\{-0.6162, 2.7184\}\\
L_{2,1} &= \mathrm{diag}\{0.6137, -2.6913\}\\
L_{2,2} &= \mathrm{diag}\{0.6123, -2.7060\}\\
L_{2,3} &= \mathrm{diag}\{0.6158, -2.7175\}\\
L_{3,1} &= \mathrm{diag}\{0.6114, -2.6853\}\\
L_{3,2} &= \mathrm{diag}\{0.6104, -2.7020\}\\
L_{3,3} &= \mathrm{diag}\{0.6140, -2.7145\}\\
L_{4,1} &= \mathrm{diag}\{-0.6152, 2.6905\}\\
L_{4,2} &= \mathrm{diag}\{-0.6133, 2.7064\}\\
L_{4,3} &= \mathrm{diag}\{-0.6173, 2.7205\}.
\end{aligned}
$$

Next, according to the obtained controller gains, one can see that the spatial responses of the BSES (14) and the estimation error system (15) under the composite controller (13) converge to zero gradually as depicted in Fig. 4(a) and (b). In addition, the disturbance observer is able to estimate disturbance $d_{i,t,x}$, which is shown in Fig. 4(c). Thus, the feasibility and superiority of the designed composite controller are validated through the presented results. Compared to the traditional H_∞ control strategy, the proposed CDRC scheme enables faster stabilization of the BSES (14), which is shown in Fig. 4(d). Moreover, this approach ensures that the target network satisfies the desired performance index γ. Therefore, the proposed approach demonstrates superior effectiveness.

Furthermore, to show the superiority of the proposed control strategy, a comparison of $\gamma_{\min}$ under the CDRC method and the traditional H_∞ control strategy is shown in Table I. As one can see from Table I, the values of $\gamma_{\min}$ decrease as the diagonal elements of the diffusion matrix D_1 increase. It implies that increasing the value of the diffusion matrix D_1 has a positive effect on the disturbance rejection capability of networks. When the diffusion matrix D_1 is fixed, the value of $\gamma_{\min}$ obtained under the composite control method is significantly smaller than that achieved by the traditional H_∞ control method. This indicates that the proposed method in this article provides improved system performance and exhibits superior disturbance–attenuation capability.

V. CONCLUSION

In this article, the problem of H_∞ bipartite synchronization has been addressed for a class of cooperation–competition CNNs with reaction–diffusion effects and hidden Markov switching. A CDRC strategy has been proposed to enhance the disturbance attenuation capability and synchronization performance of networks. To address the interaction topology, a structurally balanced graph has been employed, and a gauge transformation matrix has been utilized to convert the Laplacian matrix into a form that satisfies the zero-row-sum property. By constructing an appropriate Lyapunov functional, some criteria have been derived to guarantee bipartite synchronization under a prescribed H_∞ performance index.

In the future, we will explore the composite antidisturbance control method to deal with the thermal propagation control issue of semiconductor power chips subject to multiple disturbances.

REFERENCES

[1] I. Tomar, I. Sreedevi, and N. Pandey, "State-of-art review of traffic light synchronization for intelligent vehicles: Current status, challenges, and emerging trends," *Electronics*, vol. 11, no. 3, p. 465, Feb. 2022.

[2] X.-R. Zhang, Z.-L. Zhao, and T. Liu, "Finite-time consensus for high-order multiagent systems under directed communication topologies," *IEEE Trans. Autom. Control*, vol. 70, no. 12, pp. 8430–8437, Dec. 2025.

[3] S. Liu, M. Zheng, H. Du, and H. Yang, "Secure UAV-assisted communication for the power IoT: Integrating semantic communication and relays in the low-altitude intelligent network," *IEEE Trans. Ind. Informat.*, early access, Nov. 3, 2025, doi: 10.1109/TII.2025.3618116.

[4] N. Li, D. He, J. Shen, and Z. Shi, "Cluster secure synchronization of complex networks with cooperative-competitive interaction under DoS attacks," *IEEE Trans. Netw. Sci. Eng.*, vol. 13, pp. 3224–3239, 2026, doi: 10.1109/TNSE.2025.3628850.

[5] Z. Wang, L. Yan, Y. Fan, F. Wang, and H. Shen, "Switching event-triggered-based gain-scheduled control for bipartite synchronization of coupled coopetitive memristive neural networks," *IEEE Trans. Syst. Man, Cybern. Syst.*, vol. 55, no. 10, pp. 6951–6963, Oct. 2025.

[6] J. Wang, J. Ke, and J.-F. Zhang, "Differentially private bipartite consensus over signed networks with time-varying noises," *IEEE Trans. Autom. Control*, vol. 69, no. 9, pp. 5788–5803, Sep. 2024.

[7] H. Chen and B. Huang, "Fault-tolerant soft sensors for dynamic systems," *IEEE Trans. Control Syst. Technol.*, vol. 31, no. 6, pp. 2805–2818, Nov. 2023.

[8] H. Ye, Y. Song, Z. Zhang, and C. Wen, "Global dynamic event-triggered control for nonlinear systems with sensor and actuator faults: A matrix-pencil-based approach," *IEEE Trans. Autom. Control*, vol. 69, no. 3, pp. 2007–2014, Mar. 2024.

[9] Z. Guo, W. Wu, and G. Wu, "Full-state virtual oscillator control for grid-forming PVs to endure solar radiation and grid disturbances," *IEEE Trans. Energy Convers.*, vol. 40, no. 3, pp. 2576–2586, Sep. 2025.

[10] J. Wang, J. Wu, H. Shen, J. Cao, and L. Rutkowski, "Fuzzy H_∞ control of discrete-time nonlinear Markov jump systems via a novel hybrid reinforcement Q-learning method," *IEEE Trans. Cybern.*, vol. 53, no. 11, pp. 7380–7391, Nov. 2023.

[11] J. Wang, M. Xing, J. Cao, J. H. Park, and H. Shen, "H_∞ bipartite synchronization of double-layer Markov switched cooperation-competition neural networks: A distributed dynamic event-triggered mechanism," *IEEE Trans. Neural Netw. Learn. Syst.*, vol. 34, no. 1, pp. 278–289, Jan. 2023.

[12] M. Hua, X. Hu, F. Deng, Q. Yang, and H. Chen, "H_∞ filtering for 2-D discrete-time periodic Markov jump systems with multiplicative noise: A periodic HMM approach," *IEEE Trans. Cybern.*, vol. 55, no. 9, pp. 4196–4207, Sep. 2025.

[13] Z. Xiao, M. Zhang, H. Rao, C. Liu, and Y. Xu, "Anti-quasisynchronization for asynchronous Leader–Follower Markovian neural networks with hidden Markov model-based intermittent control," *IEEE Trans. Cybern.*, vol. 55, no. 9, pp. 4170–4181, Sep. 2025.

[14] C. E. Puerto-Santana, P. Larrañaga, and C. Bielza, "Feature saliencies in asymmetric hidden Markov models," *IEEE Trans. Neural Netw. Learn. Syst.*, vol. 35, no. 3, pp. 3586–3600, Mar. 2024.

[15] D. Wang and S. Xu, "Disturbance observer-based H_∞ control for interval type-2 fuzzy hidden Markov jump systems subject to deception attacks," *IEEE Trans. Cybern.*, vol. 54, no. 10, pp. 5843–5851, Oct. 2024.

[16] H. Shen, X. Wang, P. Duan, J. Cao, and J. Wang, "H_∞ bipartite synchronization control of Markov jump cooperation–competition networks with reaction–diffusions," *IEEE Trans. Cybern.*, vol. 53, no. 10, pp. 6626–6635, Oct. 2023.

[17] C. Huang, X. Zhang, H.-K. Lam, and S.-H. Tsai, "Synchronization analysis for nonlinear complex networks with reaction-diffusion terms using fuzzy-model-based approach," *IEEE Trans. Fuzzy Syst.*, vol. 29, no. 6, pp. 1350–1362, Jun. 2021.

[18] W.-J. Zhou, K.-N. Wu, and Y.-G. Niu, "Robust sliding mode boundary stabilization for uncertain delay reaction–diffusion systems," *IEEE Trans. Autom. Control*, vol. 70, no. 1, pp. 549–556, Jan. 2025.

[19] R. Chaibi, H. El Aiss, A. El Hajjaji, and A. Hmamed, "Stability analysis and robust H_∞ controller synthesis with derivatives of membership functions for T-S fuzzy systems with time-varying delay: Input-output stability approach," *Int. J. Control, Autom. Syst.*, vol. 18, no. 7, pp. 1872–1884, Jul. 2020.

[20] Y. Wu, Z. Guo, L. Xue, C. K. Ahn, and J. Liu, "Stabilization of complex networks under asynchronously intermittent event-triggered control," *Automatica*, vol. 161, Mar. 2024, Art. no. 111493.

[21] N. Sarrafan, J. Zarei, and M. Saif, "Improved finite-time disturbance observer-based control of networked nonholonomic high-order chained-form systems," *IEEE Trans. Syst. Man, Cybern. Syst.*, vol. 53, no. 9, pp. 5442–5453, Sep. 2023.

[22] H.-S. Lee, J. Back, and C.-S. Kim, "Disturbance observer-based robust controller for a multiple-electromagnets actuator," *IEEE Trans. Ind. Electron.*, vol. 71, no. 1, pp. 901–911, Jan. 2024.

[23] H. J. Kim and S. J. Yoo, "Disturbance observer-based adaptive chainlike filter approach for prescribed-time consensus tracking of nonlinear multiagent systems via dynamic state and input triggering," *IEEE Trans. Cybern.*, vol. 55, no. 8, pp. 4001–4014, Aug. 2025.

[24] G. Qi, J. Hu, L. Li, and K. Li, "Integral compensation function observer and its application to disturbance-rejection control of QUAV attitude," *IEEE Trans. Cybern.*, vol. 54, no. 7, pp. 4088–4099, Jul. 2024.

[25] H. Shen, X. Wang, J. Wang, J. Cao, and L. Rutkowski, "Robust composite H_∞ synchronization of Markov jump reaction–diffusion neural networks via a disturbance observer-based method," *IEEE Trans. Cybern.*, vol. 52, no. 12, pp. 12712–12721, Dec. 2022.

[26] J. Wang, D. Wang, H. Yan, and H. Shen, "Composite antidisturbance control for hidden Markov jump systems with multi-sensor against replay attacks," *IEEE Trans. Autom. Control*, vol. 69, no. 3, pp. 1760–1766, Mar. 2024.

[27] L. Wen et al., "Composite-observer-based adaptive consensus tracking control for nonlinear MASs with unknown control directions against deception attacks," *IEEE Trans. Cybern.*, vol. 55, no. 1, pp. 343–354, Jan. 2025.

[28] N. Zhao, D. Lun, H. Zhang, X. Zhao, and I. J. Rudas, "Composite anti-disturbance control for networked systems with disturbances and actuator attacks via event-triggered output feedback," *IEEE Trans. Cybern.*, vol. 56, no. 1, pp. 393–403, Jan. 2026.

[29] X. Gong, Y. Cui, J. Shen, Z. Shu, and T. Huang, "Distributed prescribed-time interval bipartite consensus of multi-agent systems on directed graphs: Theory and experiment," *IEEE Trans. Netw. Sci. Eng.*, vol. 8, no. 1, pp. 613–624, Jan. 2021.

[30] G. Cui, H. Xu, S. Xu, and J. Gu, "Predefined-time adaptive fuzzy bipartite consensus control for multiquadrotors under malicious attacks," *IEEE Trans. Fuzzy Syst.*, vol. 32, no. 4, pp. 2187–2197, Apr. 2024.

[31] L. Shi, W. Li, M. Shi, K. Shi, and Y. Cheng, "Opinion polarization over signed social networks with quasi-structural balance," *IEEE Trans. Autom. Control*, vol. 68, no. 11, pp. 6867–6874, Nov. 2023.

[32] H. Chaocheng et al., "Involution-cooperation-lying flat game on a network-structured population in the group competition," *IEEE Trans. Computat. Social Syst.*, vol. 11, no. 2, pp. 2160–2178, Apr. 2024.

[33] K. Yong, M. Chen, Y. Shi, and Q. Wu, "Flexible performance-based robust control for a class of nonlinear systems with input saturation," *Automatica*, vol. 122, Dec. 2020, Art. no. 109268.

[34] W. Qi, X. Teng, J. H. Park, J. Cao, H. Yan, and J. Cheng, "Dynamic protocol-based control for hidden stochastic jump multiarea power systems in finite-time interval," *IEEE Trans. Cybern.*, vol. 55, no. 3, pp. 1486–1496, Mar. 2025.

Xuelian Wang received the M.S. degree in control theory and control engineering from Anhui University of Technology, Ma'anshan, China, in 2021. She is currently pursuing the Ph.D. degree with the School of Mechatronic Engineering and Automation, Shanghai University, Shanghai, China.

Her current research interests include reaction–diffusion neural networks, Markov jump systems, bipartite synchronization, and fuzzy systems and control.

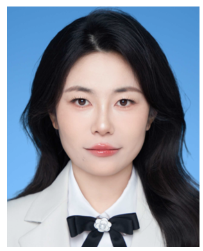

Lin Sun received the M.S. degree in control science and engineering from the School of Electrical and Information Engineering, Anhui University of Technology, Ma'anshan, China, in 2022. She is currently pursuing the Ph.D. degree in control science and engineering with the School of Electrical and Information Engineering, Tianjin University, Tianjin, China.

Her current research interests include multiagent systems, autonomous clusters, robust control, and resilient control.

Yu-Long Wang (Senior Member, IEEE) received the B.Sc. degree in computer science and technology from Liaocheng University, Liaocheng, China, in 2000, and the M.Sc. and Ph.D. degrees in control science and engineering from Northeastern University, Shenyang, China, in 2006 and 2008, respectively.

He was a Post-Doctoral Research Fellow and a Research Fellow with the Central Queensland University, North Rockhampton, QLD, Australia, an Academic Visitor with the University of Adelaide, Adelaide, SA, Australia, and a Professor with Jiangsu University of Science and Technology, Zhenjiang, Jiangsu, China. In 2017, he was appointed as an Eastern Scholar by the Municipal Commission of Education, Shanghai, China, and joined Shanghai University, Shanghai, where he is currently a Professor. His current research interests include networked control systems and motion control for marine vehicles.

Tek Tjing Lie (Life Senior, IEEE) received the B.S. degree in electrical engineering from Oklahoma State University, Stillwater, OK, USA, in 1986, and the M.S. and Ph.D. degrees in electrical engineering from Michigan State University, East Lansing, MI, USA, in 1988 and 1992, respectively.

He is a Full Professor and the Head of the School of Engineering, Computer and Mathematical Sciences, Auckland University of Technology, Auckland, New Zealand. His research interests include power system operation and control, deregulated electrical power markets, AI applications to power systems, power electronics, renewable energy, and smart grids.